agronomy

MDPI

Article

Spatiotemporal Dynamics of Climate Potential Productivity of Agricultural Ecosystems in Liaoning Province, China, During 1950–2023

Di Shi [1], Shuai Wang [1,*], Qianlai Zhuang [2], Zijiao Yang [1], Yan Wang [3] and Xinxin Jin [1]

[1] College of Land and Environment, Shenyang Agricultural University, Shenyang 110866, China; 2023220484@stu.syau.edu.cn (D.S.); 2017500046@syau.edu.cn (Z.Y.); jinxinxin0218@syau.edu.cn (X.J.)
[2] Department of Earth, Atmospheric, and Planetary Sciences, Purdue University, West Lafayette, IN 47907, USA; qzhuang@purdue.edu
[3] College of Tourism and Geography, Jiujiang University, Jiujiang 332005, China; 6180080@jju.edu.cn
* Correspondence: shuaiwang666@syau.edu.cn; Tel.: +86-24-8848-7155

Abstract

Global climate change has profoundly affected agricultural ecosystems by altering the spatiotemporal patterns of temperature and precipitation, disrupting ecological equilibrium, and increasing environmental variability for crop growth, thereby posing significant challenges to food security. Based on 1 km-resolution gridded datasets of mean precipitation and temperature for Liaoning Province from 1950 to 2023, this study integrated the Miami and Thornthwaite Memorial models with climate tendency rate analysis, Mann–Kendall trend tests, and inverse distance weighting interpolation to assess spatiotemporal changes in climate potential productivity (CPP) and its relationship with grain yield dynamics. The results show that, from 1950 to 2023, annual precipitation exhibited a fluctuating downward trend (−8.5 mm/10a), while mean annual temperature increased significantly (0.3 °C/10a). Consequently, precipitation-based climatic production potential declined at a rate of 10.4 $g \cdot m^{-2} \cdot (10a)^{-1}$, whereas temperature-based, evapotranspiration-based, and standard climate potential productivity (Yb) increased at rates of 23.3-, 6.6-, and 5.7 $g \cdot m^{-2} \cdot (10a)^{-1}$, respectively. Spatially, CPP displayed a distinct gradient characterized by higher values in the southeast and lower values in the northwest, with a stronger correlation to precipitation than to temperature. Climate classification analysis indicated that warm-humid conditions enhanced CPP, whereas cold-dry, cold-humid, and warm-dry conditions reduced productivity. Although grain yield per unit area and climate resource utilization efficiency increased by 89.4 $g \cdot m^{-2} \cdot (10a)^{-1}$ and 9.0% per decade, respectively, the yield-increasing potential declined by 84.1 $g \cdot m^{-2} \cdot (10a)^{-1}$, indicating that while advances in agricultural technology have improved resource conversion efficiency, the potential for further yield gains through climate-dependent strategies alone is increasingly limited.

Keywords: climate change; climate potential productivity; Thornthwaite Memorial model

Academic Editor: Arnd Jürgen Kuhn

Received: 9 October 2025
Revised: 18 November 2025
Accepted: 21 November 2025
Published: 23 November 2025

Citation: Shi, D.; Wang, S.; Zhuang, Q.; Yang, Z.; Wang, Y.; Jin, X. Spatiotemporal Dynamics of Climate Potential Productivity of Agricultural Ecosystems in Liaoning Province, China, During 1950–2023. *Agronomy* **2025**, *15*, 2697. https://doi.org/10.3390/agronomy15122697

1. Introduction

The World Meteorological Organization (WMO) confirms that 2024 marked the warmest year on record, with global temperatures reaching approximately 1.55 °C above

pre-industrial levels [1]. Agriculture is one of the most climate-sensitive sectors, and climate change has exerted substantial impacts on agricultural systems and food production, particularly through rising global temperatures [2,3]. The increasing frequency and intensity of extreme weather events, along with more severe natural disasters, may lead to structural shifts in agriculture and reductions in crop yields. Given that China's per capita cultivated land area is only 0.08 hm^2, climate change poses a serious threat to national food security [4,5]. As a result, the impact of climate change on agricultural productivity has become a critical issue for researchers, governments, and policymakers worldwide [6].

Liaoning Province, situated in the southern part of Northeast China, has a temperate monsoon climate marked by four distinct seasons and summer-concentrated precipitation. This climate exhibits typical characteristics of the temperate monsoon zone while also displaying notable regional variations. The province's diverse topography—comprising mountains, plains, hills, and coastal tidal flats—supports a rich and varied natural ecosystem. Liaoning is recognized as one of China's ecologically sensitive regions [7–9]. Against the backdrop of global warming, climate change not only alters the spatiotemporal patterns of temperature and precipitation but also influences vegetation growth and the structure and function of ecosystems such as forests and wetlands. These changes lead to environmental fluctuations in certain areas and have measurable impacts on agricultural production. Agriculture plays a vital role in Liaoning's economy, serving as a key national grain production base with consistently high and stable yields. Major crops include corn, rice, and soybeans. Agricultural output in the province generally meets local food demand and contributes significantly to national food security. Under the national food security strategy, Liaoning has consistently prioritized agricultural development, strengthened farmland water conservancy infrastructure, promoted the application of agricultural science and technology, and effectively responded to challenges posed by natural disasters. As a result, stable grain production in Liaoning holds substantial strategic importance for ensuring national food security. Investigating the dynamic changes in climate potential productivity in Liaoning can provide a scientific foundation and valuable insights for building a high-quality, high-yield, efficient agricultural system.

Climate potential productivity refers to the maximum biological or agricultural yield per unit area of land that can be achieved under optimal conditions—such as ideal soil quality, nutrient availability, and carbon dioxide concentration—when climate resources including solar radiation, thermal energy, and water are fully utilized [10,11]. Agriculture is one of the sectors most vulnerable to climate change, which profoundly alters agricultural systems and food production, especially in the context of global warming [12,13]. Under a changing climate, the increasing frequency and intensity of extreme weather events may disrupt cropping patterns and lead to reductions in grain output. Given that China's per capita arable land is only 0.08 hectares, climate change poses a significant threat to national food security [14,15]. Climate potential productivity represents the upper limit of crop yield that a region's climatic conditions can theoretically support, while the gap between actual yields and this potential reveals opportunities for improvement. By analyzing the relationship between actual and potential productivity, researchers can assess the theoretical capacity of climate resources to support increased grain production and identify key limiting factors—such as inadequate heat accumulation, water deficits, and declining soil fertility—using meteorological data models and crop growth simulation systems. This analysis provides a scientific basis for formulating targeted strategies to improve agricultural technologies and optimize resource allocation, both of which are critical for ensuring sustained increases in regional and national grain production capacity.

Numerous researchers have conducted theoretical and empirical analyses of climate potential productivity from diverse perspectives. Constantinidou et al. [16] assessed the impact of climate change on winter wheat yields in the eastern Mediterranean and the Middle East. I.Y. Savin et al. [17] modeled the potential yield of winter wheat in the European part of Russia using GIS and the WOFOST crop growth simulation model, finding that under current climatic conditions, overall winter wheat production in Russia could increase by 70%. Radivoje Jevtić et al. [18] evaluated the capacity of regression models to predict yield losses by incorporating both biotic and abiotic factors as predictors. Lu et al. [19] analyzed the effects of mean temperature and precipitation on climatic production potential in Heilongjiang Province and concluded that precipitation is the primary limiting factor for crop productivity in the region. Du et al. [20] found that from 1961 to 2010, the average grain production potential in the Sanjiang Plain exhibited a fluctuating upward trend, albeit with low stability due to frequent and pronounced variations. Wang et al. [21] investigated changes in climate potential productivity in the Dongting Lake Basin—a key grain-producing region—between 2000 and 2020, reporting an average annual increase of 83.7 kg $ha^{-1}a^{-1}$. Research on climate potential productivity originated in the mid-1960s to mid-1970s [22,23], during which several mature analytical models were developed. Currently, widely used models such as the Miami model [24], Thornthwaite Memorial model [25,26], AEZ model [27], and Chikugo Model [28,29] have provided critical theoretical foundations for this field of study.

The main objectives of this study are as follows: (1) to estimate the climatic productivity potentials associated with temperature, precipitation, and evapotranspiration in Liaoning Province from 1950 to 2023, using annual average temperature and precipitation grid data based on the Miami and Thornthwaite Memorial models; (2) to investigate the spatiotemporal patterns of climate-related productivity potential in the region through integrated methods including trend analysis of climatic variables, and the non-parametric Mann–Kendall (M-K) test; and (3) to evaluate the maximum potential for agricultural productivity and quantify the yield gap between current actual yields and estimated potential yields, thereby identifying opportunities for grain production enhancement. The findings provide a scientific foundation for assessing regional agricultural production capacity and improving grain output efficiency under changing climatic conditions, supporting the development of adaptive strategies in response to climate change.

2. Materials and Methods

2.1. Study Area

Liaoning Province, located in northeastern China, covers a total area of approximately 148,700 square kilometers (Figure 1). The terrain gradually slopes from the northeast to the southwest, forming a distinct topographic gradient. As a key grain-producing region in China, Liaoning primarily cultivates major crops such as corn, rice, and soybeans, with agriculture constituting a vital component of the provincial economy. Liaoning Province, as one of China's major grain-producing regions, is highly vulnerable to extreme weather events that can significantly disrupt agricultural production. Since the 1980s, numerous areas within the province have frequently, suffered from disasters caused by extreme climatic conditions. In 2007, an exceptional blizzard struck the region, causing severe agriculture, fisheries, industry, transportation, and local livelihoods, with direct economic losses amounting to approximately 14.59 billion yuan. In 2009, an unprecedented heatwave hit western Liaoning, where prolonged high temperatures coupled with insufficient rainfall led to total crop failure across extensive farmland, exacerbating regional food security concerns [30]. The province hosts diverse soil types, including brown earth and black soil, which support a varied and resilient agricultural planting structure. Situated within the temperate monsoon climate zone, Liaoning experiences

strong influences from the East Asian monsoon, resulting in pronounced seasonal contrasts and a favorable coincidence of rainfall and heat during the growing season. This climatic characteristic underpins the prevalence of typical rain-fed agriculture. Overall, the climatic conditions in Liaoning are highly conducive to the cultivation of temperate crops, providing an essential natural resource foundation for sustainable agricultural production.

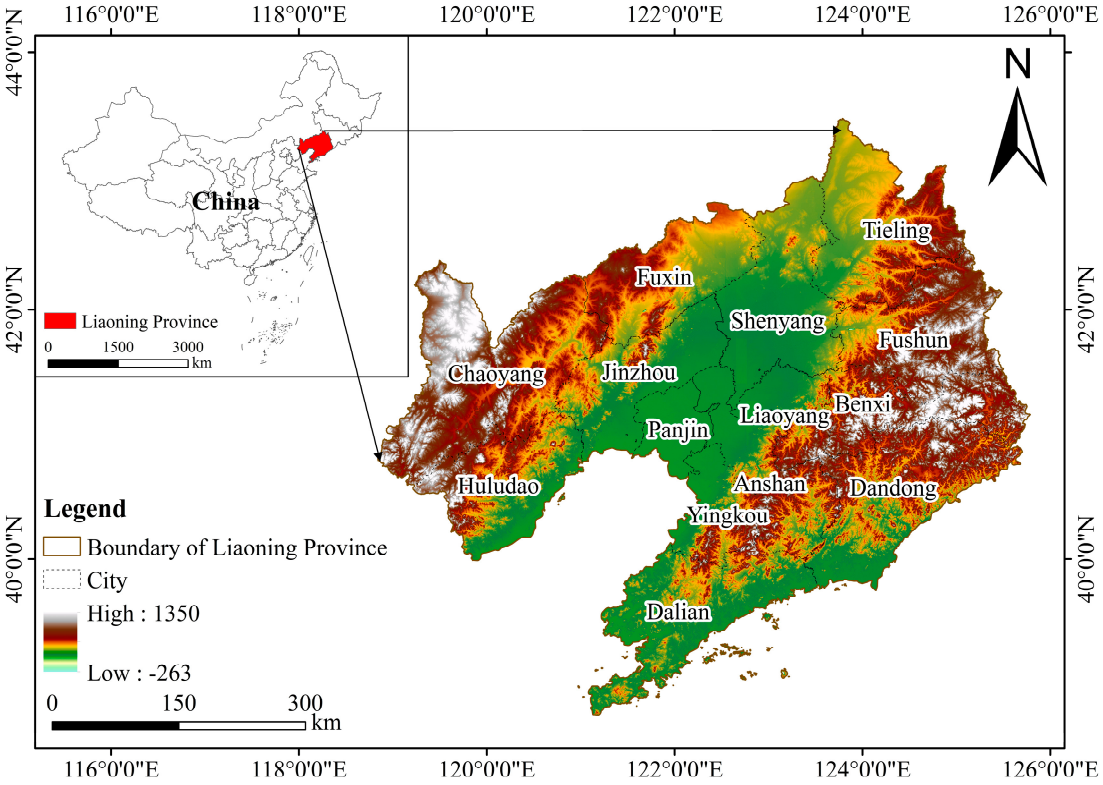

Figure 1. Study area of Liaoning Province, China.

2.2. Data Source

The dataset utilized in this study comprises meteorological data, administrative boundary data for Liaoning Province, and grain yield per unit area data for the region. Meteorological data include annual average temperature and annual average precipitation, which are reanalysis products. The original temperature data consists of monthly average temperature grids for China with a spatial resolution of 1 km, stored in NETCDF format (.nc files), referenced to WGS84 coordinate system, and recorded in units of 0.1 °C. In this study, the raster calculator tool in ArcGIS 10.8 (Esri, Redlands, CA, USA) was used to compute annual mean temperatures by averaging the 12 monthly values for each calendar year, resulting in annual temperature raster datasets. These were subsequently cropped to extract temperature data specific to Liaoning Province. Data source: https://data.tpdc.ac.cn/zh-hans/data/71ab4677-b66c-4fd1-a004-b2a541c4d5bf.3 (accessed on 15 September 2025). This gridded temperature dataset has been widely used in regional climate change studies and has been applied to assess climate change trends over the Loess Plateau [31]. The original precipitation data comprise monthly precipitation totals for China at a 1 km spatial resolution, also in NETCDF (.nc) format and referenced to the WGS84 coordinate system. Annual precipitation accumulations were derived by summing the monthly values for each year using the Raster Calculator in ArcGIS 10.8, followed by cropping to obtain data for Liaoning Province. Data source: https://data.tpdc.ac.cn/zh-hans/data/faae7605-a0f2-4d18-b28f-5cee413766a2/ (accessed on 15 September 2025). Consistent with the temperature dataset, this precipitation grid data

has also been utilized in previous studies to support climate trend analysis [31]. The administrative boundary data for Liaoning Province were obtained from National Geomatics Center of China (Beijing, China), provided in GeoJSON format, with approval number GS(2024)0650, and based on the GCS_WGS_1984 coordinate system. Grain yield per unit area data for Liaoning Province were collected from the National Bureau of Statistics of China (Beijing, China). Source: https://data.stats.gov.cn (accessed on 25 September 2025). Grain yield per unit area represents the actual harvest obtained from each unit of cultivated land, converted from the original statistical unit (kg/hm^2) to g/m^2 using a conversion factor of 1 kg/hm^2 = 0.1 g/m^2 to ensure consistency in measurement.

2.3. Methods

2.3.1. Climate Potential Productivity Model

(1) Miami model

Based on the two key climatic factors—temperature and precipitation—that influence plant growth and biomass formation, climate potential productivity is calculated to derive temperature-related and precipitation-related production potentials. Adams et al. [32] provided an in-depth discussion on simulating climate potential productivity using various methods. Among these, the Miami model is an empirical approach that establishes relationships between annual mean temperature and annual mean precipitation [33]. The Miami model is applicable to agricultural ecosystems. The light-temperature potential index is suitable for characterizing the production potential of irrigated farmland, whereas the climate potential index better represents the production potential of rain-fed farmland [34]. By integrating the Miami model and water-heat factors, it becomes feasible to estimate the natural productivity distribution of both global farmland and globally suitable uncultivated land. Subsequently, the yield distribution of such uncultivated land can be derived using the global average economic coefficient, followed by regional statistical aggregation [24]. Although it lacks detailed mechanistic processes, it is valued for its simplicity and relative accuracy, and has been widely applied in ecological and agricultural studies [35]. The calculation equations are given in Equations (1) and (2).

$$Yt = \frac{3000}{1 + e^{1.315 - 0.119t}} \quad (1)$$

$$Yr = 3000(1 - e^{-0.000664r}) \quad (2)$$

where t denotes the annual average temperature (°C); r represents the annual precipitation (mm); Yt and Yr denote the temperature-induced and precipitation-induced production potentials [kg·hm^{-2}·a^{-1}], respectively; and 3000 refers to the maximum annual dry matter yield (kg·hm^{-2}) of natural vegetation per unit area on Earth, derived from statistical data.

(2) Thornthwaite Memorial model

The potential for evapotranspiration is estimated through a functional relationship with key environmental factors such as temperature, precipitation, and vegetation cover [36]. Compared to the Miami model, which accounts solely for temperature and precipitation, the core advantage of this model is its incorporation of the key variable "actual evapotranspiration." By simultaneously calculating both potential and actual evapotranspiration, the model integrates multiple climatic factors—such as solar radiation, temperature, precipitation, saturation deficit, and wind speed—thereby providing a more accurate representation of the actual process of crop water consumption and yield formation [37]. The corresponding calculation formulas are provided in Equations (3)–(5).

$$Ye = 3000[1 - e^{-0.0009695(V-20)}] \quad (3)$$

$$V = \frac{1.05r}{\sqrt{1 + \left(\frac{1.05r}{L}\right)^2}} \quad (4)$$

$$L = 300 + 25t + 0.05t^3 \quad (5)$$

where t denotes the annual average temperature (°C); r represents the annual precipitation (mm); Ye indicates the evapotranspiration production potential [kg·hm^{-2}·a^{-1}]; V stands for the actual annual average evapotranspiration (mm), L refers to the annual maximum evapotranspiration (mm), 1.05 is a correction coefficient accounting for precipitation-evapotranspiration relationship, while the constants 300, 25, and 0.05 are empirical parameters used to estimate maximum evapotranspiration based on temperature.

2.3.2. Standard Climate Potential Productivity (Yb)

The standard climate potential productivity is defined as the minimum value among temperature-based, precipitation-based, and evapotranspiration-based climatic potential productivities. According to Liebig's Law of the Minimum, the climatic potential productivity of a region is determined by the lowest value among the calculated temperature production potential, precipitation production potential, and evapotranspiration production potential [38]. The corresponding calculation formula is presented in Equation (6).

$$Y_b = min(Y_t, Y_r, Y_e) \quad (6)$$

2.3.3. Climate Resource Utilization Efficiency

Climate resource utilization efficiency refers to the ratio of the actual grain yield per unit area in a given region to the climate potential productivity, expressed as a percentage [39]. The calculation formula is presented in Equation (7).

$$CRUE = 100\% \times Agp/CPP \quad (7)$$

where CRUE represents climate resource utilization efficiency (expressed as a percentage), Agp is actual grain yield per unit area, calculated from field survey data and from statistical yearbook records; and CPP represents climate potential productivity, estimated using the Miami model and the Thornthwaite Memorial Model described in Section 2.3.

2.3.4. Estimation of Potential for Grain Production Increase

A better understanding of the potential for increased production and its spatial distribution can help government agencies, policymakers, farmers, and other stakeholders effectively guide agricultural production. Climate potential productivity refers to the maximum yield per unit area that cultivated land can achieve under optimal conditions, through the full utilization of resources such as sunlight, water, and soil as well as favorable terrain conditions [40,41]. This study estimates the potential for grain production increase by calculating the difference between climate potential productivity and actual yield [42,43]. The specific formula is presented in Equation (8):

$$Y = CPP - AP \quad (8)$$

where Y represents the total potential for increased production (in g·m^{-2}); CPP denotes climate potential productivity (ing·m^{-2}); and AP refers to the actual productivity.

2.3.5. Mann–Kendall Trend Analysis

The Mann–Kendall (MK) trend analysis is appropriate for detecting continuous increasing or decreasing trends in time series data. It is robust against a small number of outliers and applicable to datasets that do not conform to a specific distribution, such as those in hydrology and meteorology. Additionally, it is computationally straightforward [44,45]. The MK test has been extensively employed by researchers to examine temporal trends in various climatic and hydrological variables [46,47], and can be computed using Equations (9)–(11).

$$S = \sum_{k=1}^{n-1} \sum_{j=k+1}^{n} \mathrm{Sgn}(X_j - X_k) \tag{9}$$

$$\mathrm{Sgn}(X_j - X_k) = \begin{cases} +1 & (X_j - X_k) > 0 \\ 0 & (X_j - X_k) = 0 \\ -1 & (X_j - X_k) < 0 \end{cases} \tag{10}$$

$$Z = \begin{cases} \dfrac{S-1}{\sqrt{\mathrm{Var}(S)}} & S > 0 \\ \dfrac{S+1}{\sqrt{\mathrm{Var}(S)}} & S < 0 \end{cases} \tag{11}$$

where S represents the Mann–Kendall test statistic for trend; n denotes the number of data points in the time series; k and j are indices used to iterate over the data points ($j > k$ to ensure each pair is compared once); X_j and X_k refer to the data values at positions j and k in the time series, respectively; Z represents the standardized Mann–Kendall test statistic used to assess trend significance.

To avoid inflated significance due to serial correlation in annual climate/CPP series, we applied Trend-Free Pre-Whitening (TFPW) prior to Mann–Kendall (MK) tests. Autocorrelation was first assessed using the autocorrelation function (ACF) and Ljung–Box test in R 4.3.2 (R Foundation for Statistical Computing, Vienna, Austria); for autocorrelated series, linear trends were removed, followed by elimination of residual autocorrelation using an AR(1) model. The MK test was then performed on the TFPW-processed data. For multiple series, the Holm-Bonferroni correction was applied to control the family-wise error rate: raw p-values were sorted and compared against adjusted significance thresholds ($\alpha = 0.05/(8 - k + 1)$), ensuring more rigorous inference. Additionally, Sen's slope estimator was used to quantify the magnitude of trends in each series. Results were interpreted in conjunction with the MK test Z-value (Ze) and a 95% confidence interval (CI: [−1.96, +1.96]) to enhance assessment of trend reliability.

3. Results

3.1. Spatio-Temporal Variation Characteristics of Climate

3.1.1. Temporal Variations in Annual Average Temperature and Annual Precipitation

As shown in the precipitation variation curve for Liaoning Province in Figure 2, annual precipitation between 1950 and 2023 ranged from 497.05 mm to 1014.43 mm, with a multi-year average of 687.41 mm. Significant interannual variability is evident, with peak precipitation recorded in 1964 (1014.43 mm) and the minimum in 2000 (497.05 mm), resulting in a difference of 517.38 mm between these extremes. Linear trend analysis reveals a fluctuating but overall downward trend in annual precipitation over the study period,

decreasing at a rate of 8.5 mm per decade. Similarly, as illustrated in the temperature variation curve in Figure 2, the annual average temperature in Liaoning Province ranged from 6.06 °C to 9.48 °C during the same period, with a long-term mean of 7.91 °C. Pronounced interannual variability is observed, with the highest temperature recorded in 2023 (9.48 °C) and the lowest in 1969 (6.06 °C), yielding a difference of 3.42 °C. Overall, the annual average temperature exhibited a fluctuating yet consistent upward trend across the 74-year period, increasing at a rate of 0.30 °C per decade.

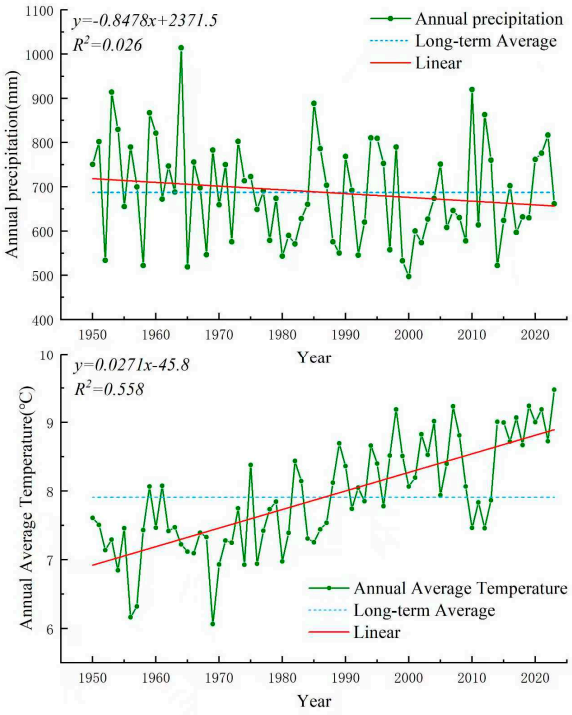

Figure 2. Interannual variations in precipitation and temperature in Liaoning Province from 1950 to 2023.

3.1.2. Spatial Variations in Annual Average Temperature and Annual Precipitation

As shown in Figure 3, the average annual precipitation generally decreases from the southeastern to the northwestern regions, while the average annual temperature tends to decrease from the southwestern to the northeastern areas. Specifically, Figure 3a illustrates that the multi-year average precipitation displays a spatial pattern increasing from the Tieling–Shenyang–Liaoyang–Anshan–Dalian axis toward both eastern and western directions. Figure 3b further reveals that the annual average temperature in Liaoning Province exhibits a latitudinal zonal distribution, decreasing from south to north and from west to east.

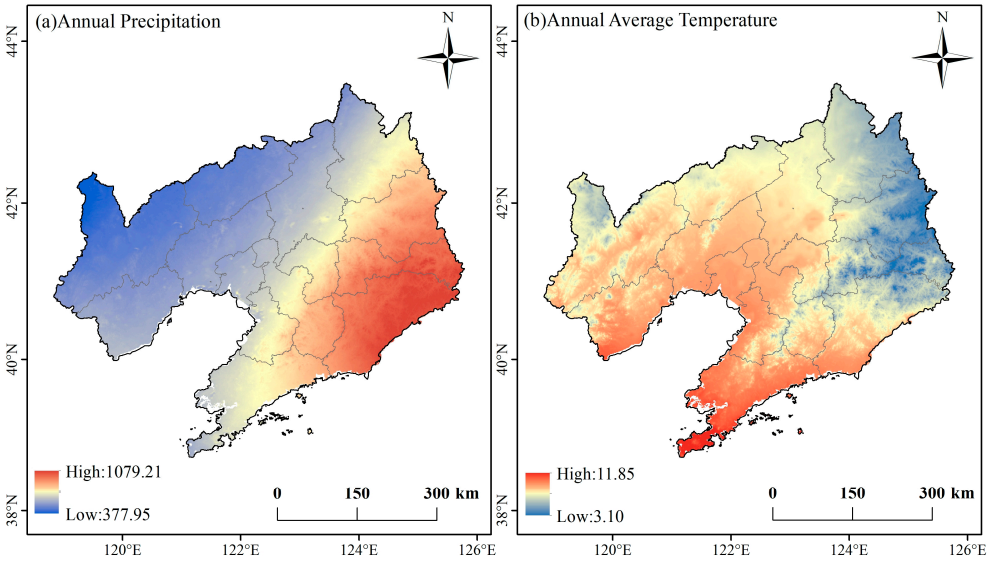

Figure 3. Spatial distribution of annual precipitation and average annual temperature in Liaoning Province from 1950 to 2023.

3.2. Spatio-Temporal Variation Characteristics of Climate Potential Productivity

3.2.1. Temporal Variation Characteristics of Climate Potential Productivity

From 1950 to 2023, precipitation climate potential productivity (Yr) in Liaoning Province exhibited notable interannual variability, with a long-term average of 1063.3 $g \cdot m^{-2} \cdot a^{-1}$ and a declining trend of 10.4 $g \cdot m^{-2} \cdot (10a)^{-1}$. The highest value was recorded in 1964 (1432.7 $g \cdot m^{-2}$), while the lowest occurred in 2000 (817.4 $g \cdot m^{-2}$), resulting in a difference of 615.2 $g \cdot m^{-2}$. The cumulative anomaly curve (Figure 4a) indicates an increasing trend from 1950 to 1975, followed by fluctuating decreases from 1976 to 2023. Decadal anomaly analysis (Table 1) reveals positive anomalies during 1950–1959, 1960–1969, 1990–1999, and 2010–2023, whereas negative anomalies were observed in 1970–1979, 1980–1989, and 2000–2009.

The temperature climate potential productivity (Yt) ranged from 1067.6 to 1359.9 $g \cdot m^{-2} \cdot a^{-1}$, with a multi-year average of 1223.2 $g \cdot m^{-2} \cdot a^{-1}$, increasing at a rate of 23.3 $g \cdot m^{-2} \cdot (10a)^{-1}$. The cumulative anomaly curve (Figure 4b) shows fluctuating declines from 1950 to 1987, followed by a sustained upward trend from 1988 to 2023. Decadal anomaly analysis (Table 1) reveals negative anomalies during 1950–1959, 1960–1969, 1970–1979, and 1980–1989, while positive anomalies dominated in 1990–1999, 2000–2009, and 2010–2023.

The potential productivity of climatic evapotranspiration (Ye) exhibited an increasing trend, with a decadal growth rate of 6.6 $g \cdot m^{-2} \cdot (10a)^{-1}$ and a long-term average of 966.3 $g \cdot m^{-2} \cdot a^{-1}$. The maximum value was recorded in 1952 at 1074.9 $g \cdot m^{-2}$, while the minimum occurred in 1956 at 786.9 $g \cdot m^{-2}$, resulting in a range of 288.0 $g \cdot m^{-2}$. The cumulative anomaly curve (Figure 4c) indicates fluctuating declines from 1950 to 1982, followed by a sustained increase from 1983 to 2023. Decadal anomaly analysis (Table 1) reveals negative anomalies during 1950–1959, 1960–1969, 1970–1979, 1980–1989, and 2000–2009, whereas positive anomalies were observed in 1990–1999 and 2010–2023.

The standard climate potential productivity (Yb) showed an increasing trend, with a growth rate of 5.7 $g \cdot m^{-2} \cdot (10a)^{-1}$ and a multi-year average of 958.1 $g \cdot m^{-2} \cdot a^{-1}$. The maximum value reached 1058.7 $g \cdot m^{-22}$ in 1998, while the minimum was 817.4 $g \cdot m^{-2}$ in 2000, resulting in a difference of 241.3 $g \cdot m^{-2}$. The 4-day cumulative anomaly curve declined fluctuatingly from 1950 to 1983, followed by a rising trend from 1984 to 2023. The decadal anomaly patterns are consistent with those observed in evapotranspiration and climatic production potential (Ye).

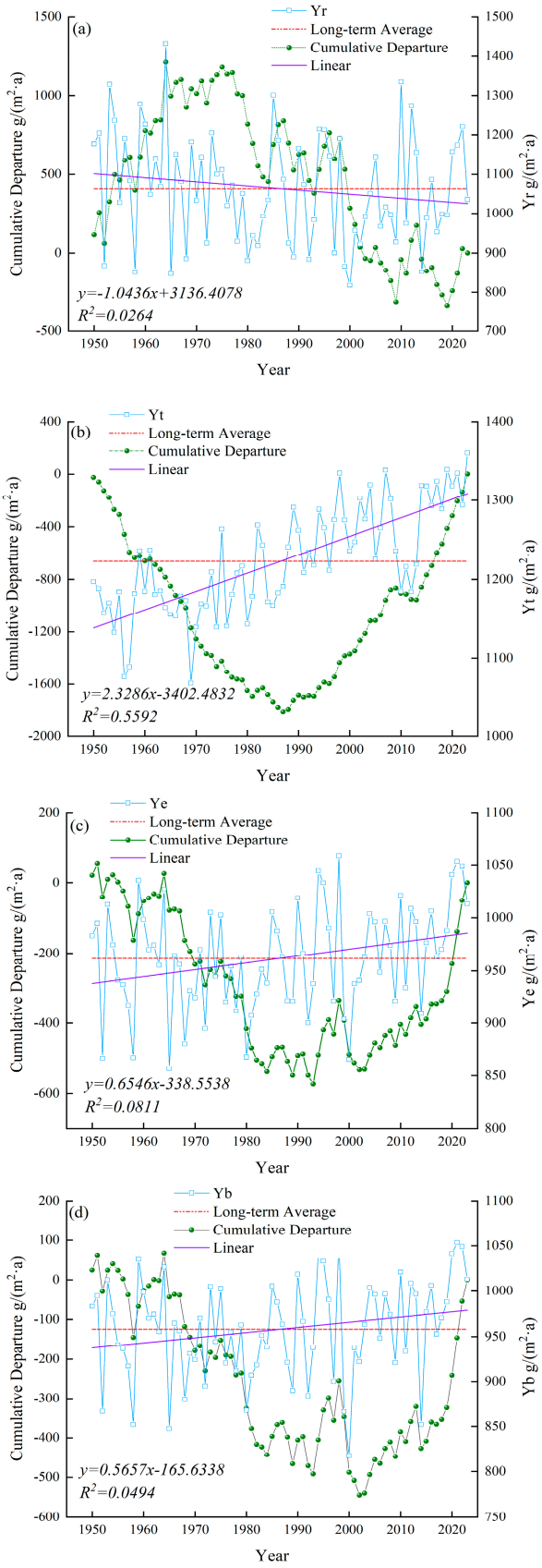

Figure 4. Interannual variation in climate potential productivity in Liaoning Province from 1950 to 2023. (**a**) Precipitation climate potential productivity (Yr); (**b**) Temperature climate potential productivity (Yt); (**c**) Potential productivity of climatic evapotranspiration (Ye); (**d**) Standard climate potential productivity (Yb).

Table 1. Annual average and anomaly trends of climate productivity in Liaoning Province from 1950 to 2023.

Decade	Precipitation Climate Potential Productivity (g·m⁻²)		Temperature Climate Potential Productivity (g·m⁻²)		Evapotranspiration Potential Productivity (g·m⁻²)		Standard Climate Potential Productivity (g·m⁻²)	
	Mean	Anomaly	Mean	Anomaly	Mean	Anomaly	Mean	Anomaly
1950–1959	1124.56	61.25	1161.23	−62.01	952.92	−8.92	951.40	−6.75
1960–1969	1106.30	43.00	1168.10	−55.13	951.35	−10.50	950.45	−7.71
1970–1979	1058.99	−4.32	1183.39	−39.85	949.05	−12.79	949.05	−9.10
1980–1989	1015.92	−47.38	1207.80	−15.43	939.13	−22.71	935.08	−23.07
1990–1999	1063.78	0.47	1257.41	34.17	977.50	15.65	970.06	11.91
2000–2009	978.99	−84.31	1274.88	51.64	954.76	−7.08	942.60	−15.56
2010–2023	1085.66	22.35	1285.11	61.87	994.95	33.10	985.55	27.40

The Mann–Kendall non-parametric test was employed to analyze temporal trends in three types of climate potential productivity and standard climate productivity (Yb) in Liaoning Province (Figure 5). For precipitation climate potential productivity, the UF statistic remained above zero (indicating an increasing trend) from 1953 to 1957, then stabilized below zero after 1958, and surpassed the critical threshold of ±1.96 in 1981, indicating a significant declining trend. The UF and UB curves intersected four times—in 1957, 1959, 1961, and 1964—suggesting possible change points; combined with a sliding t-test, a significant abrupt change was confirmed in 1964, with a mean difference of 585.2 $g \cdot m^{-2} \cdot a^{-1}$ before and after this year. For temperature climate potential productivity, the UF values were below zero (indicating a decreasing trend) during 1950–1960 and 1964–1977, then stabilized above zero after 1978, exceeding the critical value of 1.96 in 1990, which indicates a significant increasing trend. The UF and UB lines intersected only once, in 1992, but without crossing the critical threshold, suggesting no definitive mutation point. Regarding climatic evapotranspiration potential productivity, the UF statistic exceeded the ±1.96 threshold only in 2023, reflecting significant fluctuating behavior. The UF and UB lines intersected in 2018, and the sliding t-test statistic surpassed the critical value, confirming a sudden change in that year. For standard climate potential productivity (Yb), the UF values were negative (<0) in 1952, 1954–1956, and 1958–2008, reaching below −1.96 in 1957 (indicating a significant decline), while positive values (>0) occurred in 1951, 1953, and 2009–2023 (indicating an increasing trend). The UF and UB lines intersected in 2018, and the sliding t-test confirmed this year as a statistically significant breakpoint.

The Mann–Kendall test, following TFPW preprocessing and Holm-Bonferroni correction, revealed the following trends: for precipitation-based climate potential productivity (Yr), Sen's slope was −1.126 $g \cdot m^{-2} \cdot a^{-1}$ with a Z statistic of −1.251 ($|Z| < 1.96$), indicating a non-significant decreasing trend; for temperature-based climate potential productivity (Yt), Sen's slope was 2.351 $g \cdot m^{-2} \cdot a^{-1}$ and $Z = 6.813$ ($|Z| > 1.96$), indicating a statistically significant increasing trend; for evapotranspiration-based potential productivity (Ye), Sen's slope was 0.636 $g \cdot m^{-2} \cdot a^{-1}$ and $Z = 2.193$ ($|Z| > 1.96$), also showing a significant increase; and for standard climate potential productivity (Yb), Sen's slope was 0.588 $g \cdot m^{-2} \cdot a^{-1}$ with $Z = 1.904$ ($|Z| \approx 1.96$), suggesting a marginally significant upward trend.

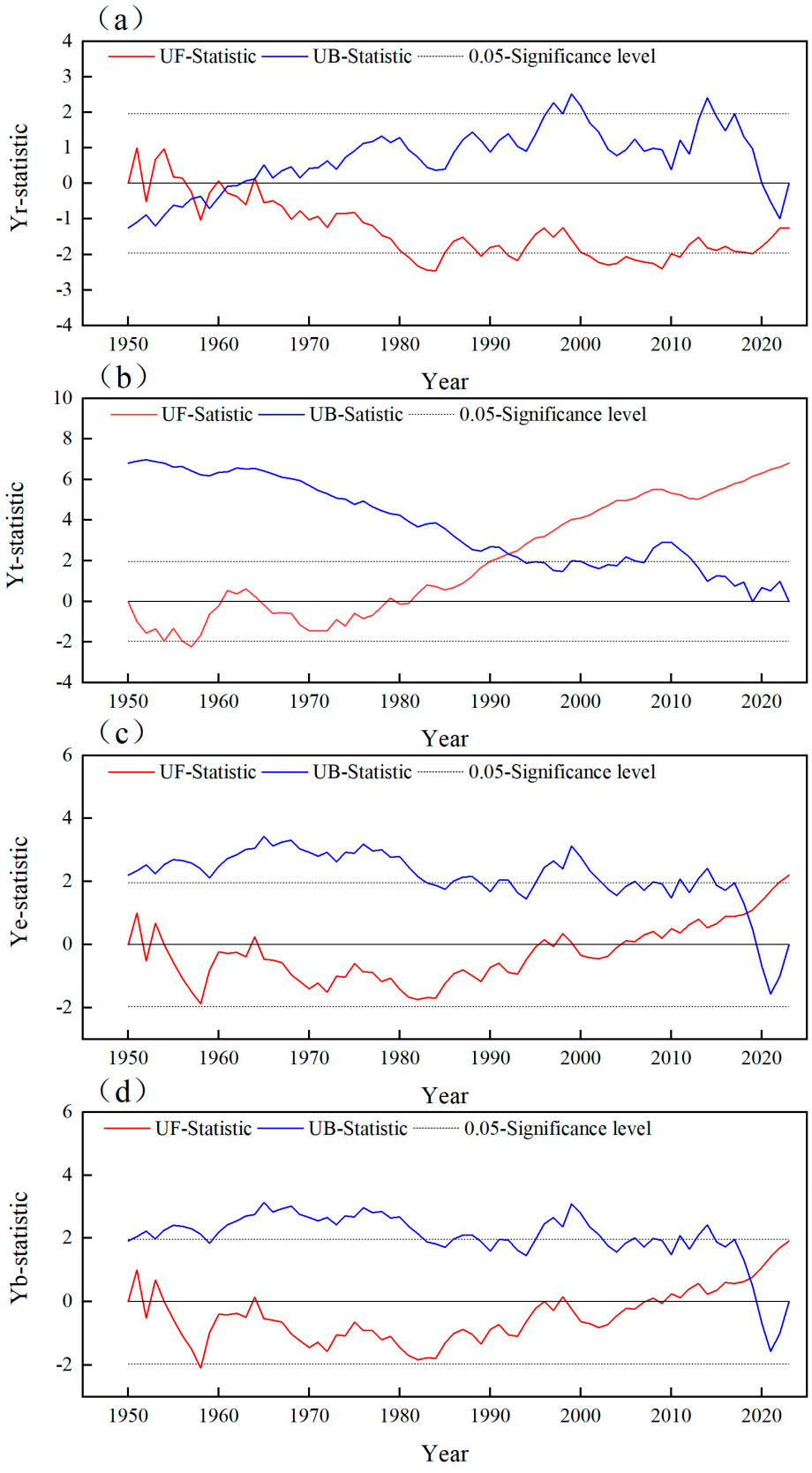

Figure 5. MK mutation test of climate potential productivity in Liaoning Province from 1950 to 2023. (**a**) MK mutation test of the precipitation climate potential productivity (Yr); (**b**) MK mutation test of the temperature climate potential productivity (Yt); (**c**) MK mutation test of the potential productivity of climatic evapotranspiration (Ye); (**d**) MK mutation test of the standard climate potential

productivity (Yb). Notes: UF (Forward Statistic): Standardized MK statistic computed from the forward time series (1950–2023); positive values (UF > 0) indicate an increasing trend, whereas negative values (UF < 0) indicate a decreasing trend. A trend is considered statistically significant when |UF| exceeds 1.96 (dashed line), corresponding to $p < 0.05$. UB (Backward Statistic) represents the standardized Mann–Kendall statistic calculated from the reversed time series (2023–1950), with the results inverted to allow direct comparison with UF.

3.2.2. Spatial Distribution Characteristics of Climate Potential Productivity

As shown in Figure 6: Precipitation climate potential productivity (Yr) exhibited the lowest values in Chaoyang City and Fuxin City, while the highest values were found in Dandong City and Benxi City. The spatial distribution pattern corresponds closely with annual average precipitation, revealing a gradual increase from the northwest to the southeast. Western Liaoning generally shows lower productivity, with Dandong and Benxi emerging as high-value zones ranging from 1362 to 1523 $g \cdot m^{-2} \cdot a^{-1}$, whereas the western parts of Chaoyang and Fuxin represent low-value areas. Regarding climatic tendency rates, the entire province displays a decreasing trend, with Dandong City showing the most significant decline at −1.8 $g \cdot m^{-2} \cdot (10a)^{-1}$.

The temperature climate potential productivity (Yt) ranges from 840 to 1571 $g \cdot m^{-2} \cdot a^{-1}$, exhibiting a spatial distribution pattern that closely aligns with the annual mean temperature, decreasing from southwest to northeast. High-value areas are primarily located in Dalian City and Huludao City, where Yt values range from 1369 to 1571 $g \cdot m^{-2} \cdot a^{-1}$, whereas low-value areas are observed in Benxi City and Fushun City, with values between 840 and 1049 $g \cdot m^{-2} \cdot a^{-1}$. Regarding the climate tendency rate, the entire province displays a positive increasing trend, with the most significant increases occurring in Huludao City and the southwestern region of Chaoyang City, reaching up to 2.8 $g \cdot m^{-2} \cdot (10a)^{-1}$.

The potential productivity of climate evapotranspiration (Ye) ranges from 735 to 1139 $g \cdot m^{-2} \cdot a^{-1}$, exhibiting a clear decreasing gradient from the southeast to the northwest. High-value regions are concentrated in Dandong City and eastern Dalian City, where Ye values range from 1037 to 1139 $g \cdot m^{-2} \cdot a^{-1}$, whereas low-value areas are primarily observed in Chaoyang City, with values between 735 and 819 $g \cdot m^{-2} \cdot a^{-1}$. In terms of the climate tendency rate, the entire province shows an overall increasing trend, with Fushun City experiencing the most pronounced increase at 1.2 $g \cdot m^{-2} \cdot (10a)^{-1}$.

The standard climate potential productivity (Yb) ranges from 704 to 1244 $g \cdot m^{-2} \cdot a^{-1}$. Spatially, Yb exhibits a distinct north–south gradient, with lower values in the north and higher values in the south, increasing from the northwest to the southeast. This pattern is consistent with Ye's findings. High-value areas are primarily concentrated in Dandong City and its surrounding regions, where Yb ranges from 1116 to 1244 $g \cdot m^{-2} \cdot a^{-1}$, whereas Chaoyang City represents a low-value zone with Yb values between 704 and 818 $g \cdot m^{-2} \cdot a^{-1}$. Regarding climatic tendency rates, northwestern Liaoning Province displays a decreasing trend, most notably in Chaoyang City, which shows the strongest decline at −1.9 $g \cdot m^{-2} \cdot (10a)^{-1}$. In contrast, southeastern Liaoning Province exhibits an increasing trend, with Dalian and Dandong cities showing the most significant rise at 1.6 $g \cdot m^{-2} \cdot (10a)^{-1}$.

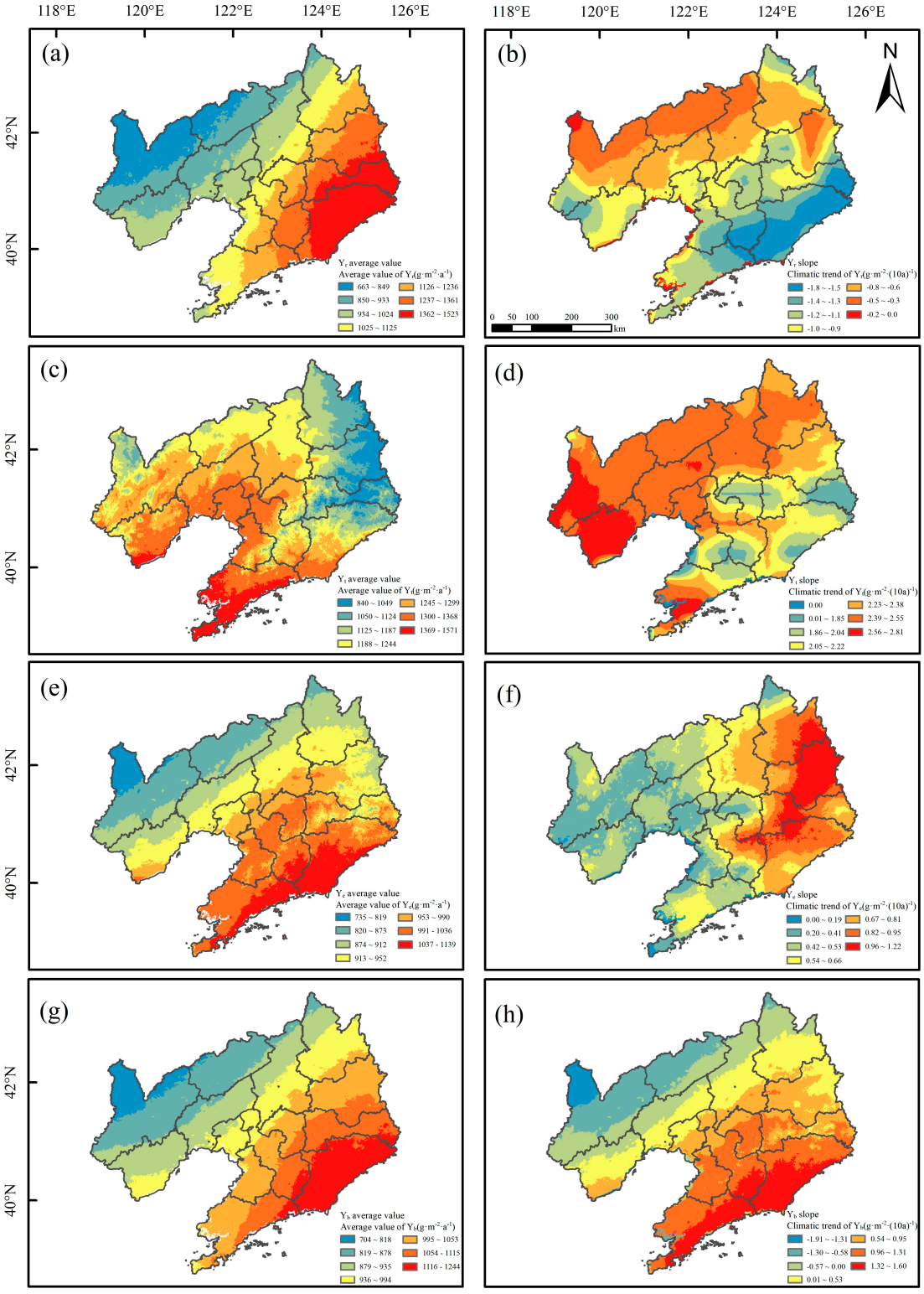

Figure 6. Annual average value of climate potential productivity and the spatial distribution of climate tendency rate in Liaoning Province. (**a**) The average precipitation-based climatic potential productivity (Yr); (**b**) The slope of precipitation-based climatic potential productivity (Yr); (**c**) The average temperature-based climatic potential productivity (Yt); (**d**) The slope of temperature-based climatic potential productivity (Yt); (**e**) The average climatic evapotranspiration potential productivity (Ye); (**f**) The slope of climatic evapotranspiration potential productivity (Ye); (**g**) The average standardized climatic potential productivity (Yb); (**h**) The slope of standardized climatic potential productivity (Yb).

3.3. Response of Liaoning Province's Standard Climate Potential Productivity to Climate Change

3.3.1. Relationship Between Meteorological Factors and Standard Climate Potential Productivity (Yb)

To investigate the relationship between standard climate potential productivity (Yb) and annual average temperature and precipitation in Liaoning Province, a time-series trend analysis of climate potential productivity, temperature, and precipitation was conducted using data from 1950 to 2023. As shown in Figure 7, both standard climate potential productivity (Yb) and temperature exhibit minor fluctuations over time and remain relatively stable. Precipitation showed a significant positive correlation with standard climate potential productivity (Yb) in Liaoning Province ($R^2 = 0.6621$, $p < 0.05$), indicating that as precipitation increased, standard climate potential productivity (Yb) exhibited a clear upward trend. In contrast, temperature showed no significant correlation with standard climate potential productivity (Yb) ($R^2 = 0.0876$, $p > 0.05$), suggesting that temperature variations had little influence on productivity under current climatic conditions.

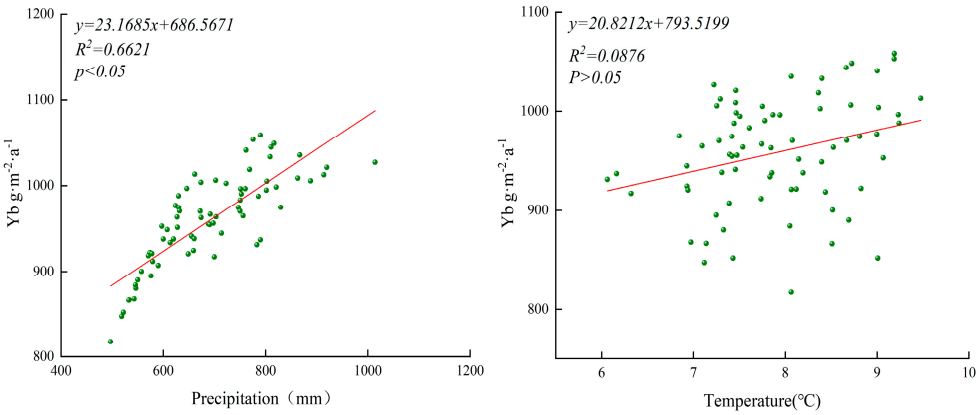

Figure 7. Relationship between the standard climate potential productivity and temperature and precipitation in Liaoning Province from 1950 to 2023.

3.3.2. Sensitivity Analysis of Standard Climate Potential Productivity to Temperature and Precipitation Variations

To analyze the synergistic effects of meteorological factors on standard climate potential productivity (Yb), we examine the quantitative relationships between Yb and two key variables—the annual average temperature and annual precipitation—and develop a multiple regression model to characterize these interactions.

$$Yb = 34.803t + 0.447R + 375.737 \ (R^2 = 0.892) \quad (12)$$

where Yb denotes the standard climate production potential ($g \cdot m^{-2}$), t represents the average annual temperature (°C), and R denotes the annual precipitation (mm). According to the analysis of variance, the F-statistic value is 303.50, with a significance probability of $p < 0.001$, indicating that the regression equation is statistically significant and exhibits a strong positive correlation. The apparently larger magnitude of the temperature coefficient (34.803) in Equation (12) stems from differences in measurement units: temperature is recorded in °C (mean 7.91 °C), while precipitation is measured in millimeters (mean 687.41 mm). The considerable disparity in scale between these variables necessitates careful interpretation, as real-world temperature fluctuations are inherently constrained.

To simulate the sensitivity of standard climate potential productivity (Yb) to changes in multi-year average temperature and precipitation, this study establishes five climate scenarios. Given that the study area is abundant in solar energy and receives sufficient

sunlight to fully meet plant growth and development requirements, standard climate potential productivity (Yb) can be estimated based on long-term average temperature and precipitation. The calculations were conducted under scenarios in which the annual mean temperature increased or decreased by 1 °C or 2 °C with constant precipitation, and in which annual precipitation increased or decreased by 10% or 20% with unchanged temperature. Changes in standard climate potential productivity (Yb) in Liaoning Province under these climate variations were then compared. As shown in Table 2, the standard climate potential productivity (Yb) in Liaoning Province varies significantly with changes in temperature and precipitation. When considering single-factor effects, an increase in temperature leads to a greater rise in Yb than an equivalent percentage increase in precipitation. Conversely, a decrease in precipitation results in a smaller reduction in Yb compared to a temperature decrease. Specifically, when temperature remains constant and precipitation increases by 10% and 20%, the provincial average standard climate potential productivity (Yb) increases by 4.5 and 9.0 $g \cdot m^{-2}$, representing increments of 0.47% and 0.93%, respectively. When precipitation decreases by 10% and 20%, the average productivity declines by 4.5 and 9.0 $g \cdot m^{-2}$, corresponding to reductions of 0.47% and 0.93%. With precipitation held constant, for every 1 °C and 2 °C increase in temperature, the provincial average standard climate potential productivity (Yb) increases by 34.8 and 69.6 $g \cdot m^{-2}$, equivalent to increases of 3.63% and 7.26%, respectively. The average standard climate potential productivity (Yb) across the province decreases by 34.8 and 69.6 $g \cdot m^{-2}$, corresponding to negative changes of 3.63% and 7.26%, respectively. This indicates that the average change in standard climate potential productivity (Yb) is positively correlated with both temperature and precipitation, with a more pronounced response to temperature.

In fact, temperature and precipitation often change simultaneously, jointly influencing Yb. When temperature increases (or decreases) by 1 °C or 2 °C and precipitation rises (or falls) by 10% or 20%, the climate is classified as "warm and humid" or "cold and dry,", respectively. Under these conditions, the magnitude of Yb change is consistent, ranging from 4.10% to 8.20%. In contrast, under "cold and wet" and "warm and dry" scenarios—where temperature decreases (or increases) by 1 °C or 2 °C and precipitation increases (or decreases) by 10% or 20%—the corresponding changes in Yb remain uniformly negative, varying between −6.80% and −2.70%.

Table 2. Changes in standard climate potential productivity under the background of variations in annual average temperature and annual precipitation in Liaoning Province.

Temperature/°C	Precipitation/ mm				
	−20	**−10**	**0**	**10**	**20**
−2	−8.20%	−7.73%	−7.26%	−6.80%	−6.33%
−1	−4.57%	−4.10%	−3.63%	−3.17%	−2.70%
0	−0.93%	−0.47%	0.00%	0.47%	0.93%
1	2.70%	3.17%	3.63%	4.10%	4.57%
2	6.33%	6.80%	7.26%	7.73%	8.20%

3.4. Estimation of Potential for Grain Production Increase and Response of Grain Output to the Standard Climate Potential Productivity

From 1950 to 2023, climate resource utilization efficiency, standard climate potential productivity (Yb), and grain yield per unit area in Liaoning Province generally showed a fluctuating but upward trend, with average increasing rates of 9.0% per decade, 5.3 $g \cdot m^{-2} \cdot (10a)^{-1}$, and 89.4 $g \cdot m^{-2} \cdot (10a)^{-1}$, respectively. In contrast, the potential for grain production growth exhibited a fluctuating yet declining trend, decreasing at an average rate of 84.1 $g \cdot m^{-2} \cdot (10a)^{-1}$ every ten years (Figure 8). The correlation coefficient between climate

resource utilization efficiency and standard climate potential productivity (Yb) was 0.0107, indicating a positive but statistically insignificant relationship. Conversely, the correlation coefficient between climate resource utilization efficiency and grain yield per unit area was 0.9839, revealing a strong and statistically significant positive association (Figure 9).

In the 1950s, the average values of standard climatic potential productivity (Yb), grain yield per unit area, climatic resource utilization efficiency, and grain yield increase potential were 951.4 g·m^{-2}·a^{-1}, 143.1 g·m^{-2}·a^{-1}, 15.1%, and 808.3 g·m^{-2}·a^{-1}, respectively. By the 2020s, these values had increased to 990.2 g·m^{-2}·a^{-1}, 652.3 g·m^{-2}·a^{-1}, 65.9%, and decreased to 337.9 g·m^{-2}·a^{-1}, respectively. Compared to the 1950s, grain yield per unit area and climatic resource utilization efficiency in the 2020s rose by 3.6-fold and 3.4-fold, respectively, while the potential for grain yield increase in the 2020s was 1.4 times lower than that observed in the 1950s (Table 3).

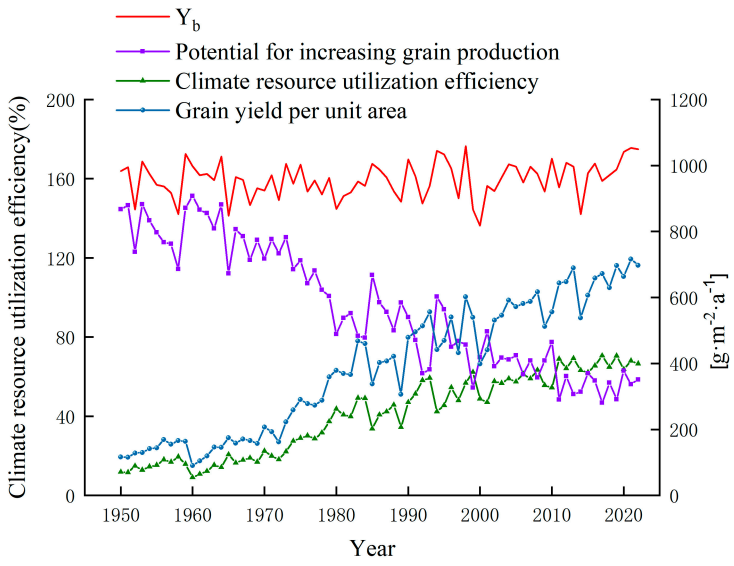

Figure 8. The climate resource utilization efficiency, standard climate potential productivity, potential for grain increase and interannual variation in grain yield per unit area from 1950 to 2023.

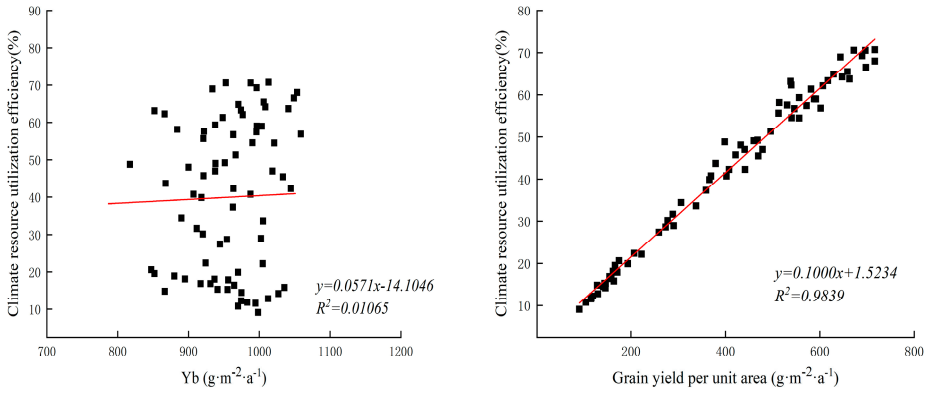

Figure 9. Correlation analysis of climate resource utilization from 1950 to 2023.

Table 3. The interdecadal variations in standard climate potential productivity, grain yield per unit area, climate resource utilization efficiency and grain increase potential.

Decade	Y_b g·m^{-2}	Grain Yield Per Unit Area g·m^{-2}	Climate Resource Utilization Efficiency (%)	Potential for Increasing Grain Production g·m^{-2}
1950–1959	951.4	143.1	15.1	808.3
1960–1969	950.4	143.4	15.2	807.0
1970–1979	949.1	253.3	26.7	695.8
1980–1989	935.1	391.9	41.9	543.2
1990–1999	970.1	507.1	52.5	463.0
2000–2009	948.1	538.0	56.6	410.1
2010–2023	990.2	652.3	65.9	337.9

Note: The period "2010–2023" covers a 14-year span, exceeding a standard decade. It is included to incorporate the most recent data available through 2023, thereby reflecting up-to-date trends. When interpreting this period, it is important to consider its extended duration relative to the conventional 10-year intervals used for other decades.

4. Discussion

4.1. Influence of Temperature and Precipitation on Yb

Research has demonstrated that temperature and precipitation are the primary climatic drivers influencing standard climate potential productivity (Yb) [48–50]. In Liaoning Province, the prevailing "warm and humid" climate conditions are particularly favorable for grain production, whereas cold and dry environments—especially low temperatures and droughts during the growing season—exert negative impacts on crop yields. Drawing on observed climate change trends in Liaoning Province and findings from existing studies [51], projections indicate that by 2050, the regional climate will shift toward a more pronounced "warm and humid" regime, with the most significant warming anticipated in southern areas. This climatic transition is expected to enhance climate potential productivity across the province. Specifically, under scenarios of a 1–2 °C temperature increase coupled with a 10–20% rise in precipitation, climate production potential could increase by 4.1–8.2%. These results suggest that future climate conditions characterized by warmth and increased humidity are likely to elevate agricultural production capacity in Liaoning Province.

Studies have also found that, compared to temperature, precipitation exerts a stronger limiting influence on climatic production potential, indicating that water availability is the primary constraint on agricultural development—a conclusion supported by additional research [52–55]. This pattern can be attributed to the climatic characteristics of Liaoning Province, located in the East Asian monsoon region and characterized by a temperate monsoon climate. Precipitation in the province is highly seasonal, with the majority concentrated in summer and significantly drier conditions during winter. As a result, agricultural production relies heavily on spring and summer rainfall, while autumn and winter droughts impose substantial stress on crop growth, particularly during critical developmental stages. During winter, low temperatures combined with limited precipitation further reduce water availability, making it insufficient to meet agricultural demands. Consequently, constraints on water resources have become a major bottleneck for economic development in Liaoning Province, especially within the agricultural sector.

In summary, while the trend of significant warming has been well established, uncertain changes in precipitation patterns will be the primary factor determining whether agricultural productivity in Liaoning Province will increase or decrease, and to what extent. To sustain agricultural output, more efficient water resource management and advanced irrigation technologies are urgently needed—particularly for water-intensive

crops such as rice and maize. Improving water use efficiency through technological innovation and mitigating the adverse effects of prolonged dry periods are critical measures for ensuring the stability and long-term sustainability of agricultural systems.

4.2. Response of Potential Grain Production Increase to Standard Climate Potential Productivity

This study utilizes standard climatic potential productivity (Yb) to calculate climate resource utilization efficiency, thereby ensuring a baseline level of climate resource use in Liaoning Province, minimizing amplitude errors arising from various influencing factors, and improving the accuracy of the final estimation. From 1960 to 1990, climate resource utilization efficiency remained relatively low, primarily due to limited technological development, inefficient fertilizer application, and inferior crop varieties. Since the 1990s, Liaoning Province has intensified efforts in agricultural technology research, development, and dissemination. Significant advancements have been achieved in high-yield crop breeding, farmland irrigation techniques, and pest and disease control, all of which have substantially enhanced agricultural production efficiency. As a result, climate resource utilization efficiency began to increase more rapidly during this period, reflecting marked progress in the application and advancement of agricultural science and technology. The analysis indicates that future improvements in efficiency depend critically on increasing grain yield per unit area—a finding consistent with the research of Jiang L et al. [56] conducted in the same region.

Since the 1990s, grain yield per unit area in Liaoning Province has increased from 507.1 $g \cdot m^{-2}$ to 652.3 $g \cdot m^{-2}$, representing a 27% rise. This improvement is primarily attributable to advances in agricultural science and technology, including the development of high-yielding crop varieties and enhanced irrigation techniques, which have collectively improved the efficiency of climate resource utilization. The correlation coefficient between climate resource utilization efficiency and standard climate potential productivity (Yb) in Liaoning Province is 0.0107, indicating a positive but statistically insignificant relationship. In contrast, the correlation coefficient between climate resource utilization efficiency and per-unit grain yield is 0.98, suggesting a strong and highly positive association. This indicates that increasing per-unit grain yield is a critical pathway for enhancing climate resource utilization efficiency. However, the standard climate potential productivity (Yb) has declined from 808.3 $g \cdot m^{-2}$ in the 1950s to 337.9 $g \cdot m^{-2}$ in the 2010s, reflecting a narrowing gap between actual yields and climatic potential. This trend suggests limited future potential for boosting grain production solely through favorable climatic conditions.

In summary, increasing grain yield per unit area is a key strategy for enhancing climate resource use efficiency, though limiting factors vary significantly across regions. Based on the spatial distribution of the standard climate potential productivity in Liaoning Province (Figure 6), region-specific measures should be implemented to maximize yield potential by addressing the distinct constraints in the northwest low-value zone and the southeast high-value zone. In the northwest, where summer precipitation is concentrated and spring droughts are frequent, the adoption of "fish-scale pits + rainwater harvesting pits" combined with small-scale drip irrigation systems can alleviate water stress during the critical maize sowing period (April–May), thereby improving yield stability in rainfed croplands. Establishing monitoring sites that integrate soil moisture and yield data will enable the development of a field water productivity metric—"kilograms of grain per cubic meter of water"—to support demand-based irrigation management and reduce. In the southeastern high-value zone (Liaohe River lower plain), where rice cultivation is intensive, replacing traditional flood irrigation with intermittent "shallow-wet-dry" irrigation, integrated with smart water-fertilizer integration systems, can maintain high yields while reducing irrigation water use by 20–25%, consistent with the goal of

high-efficiency water use in high-potential areas. In response to the regional trends of rising temperatures and lengthening growing seasons, maize planting has been shifted from mid-April to late April to avoid peak heat during late July to early August. Simultaneously, the promotion of short-maturity rice varieties helps mitigate the adverse effects of high temperatures on grain filling.

Therefore, further efforts should prioritize strengthening water conservation measures, improving agricultural water infrastructure, advancing water-saving agricultural practices, and promoting the cultivation of drought-resistant crop varieties. These actions are crucial for ensuring the sustainable development of agriculture in Liaoning Province under projected climate change scenarios and for enhancing the efficiency of climate resource utilization.

4.3. Uncertainty in Current Research

Although the Miami model and the Thornthwaite Memorial model fully account for the integrated effects of environmental factors—such as light, temperature, and water availability—on vegetation biomass accumulation, they also incorporate key physiological mechanisms of plant growth and internal energy conversion processes associated with canopy evapotranspiration and photosynthesis. These models establish a quantitative relationship between vegetation productivity and photosynthetic activity, suggesting that higher evapotranspiration rates generally correspond to increased photosynthetic efficiency and, consequently, greater biomass accumulation. By integrating evapotranspiration with meteorological variables such as temperature and precipitation, these models offer a practical approach to assessing the impacts of climate change on plant productivity. Furthermore, using regional estimates of annual climate production potential, they enable the analysis of spatio-temporal patterns in this potential, facilitating investigations into how climatic instability affects ecosystem productivity. As a result, the Miami and Thornthwaite Memorial models have become foundational tools in climate ecology for estimating terrestrial ecosystem productivity and are widely applied across diverse vegetation types [24,38]. They have significantly advanced the evaluation of climate-driven vegetation productivity, the simulation of vegetation growth dynamics, the study of interactions between terrestrial ecosystems and climate evolution, and the prediction of ecological responses to environmental change. It is important to clarify that although direct observational data on climatic potential productivity are unavailable, the reliability of our estimates is supported by two key factors: the scientific rigor of the Miami and Thornthwaite Memorial models—both grounded in plant physiological principles and extensively validated in regional studies [19,20]—and the high quality of the input climate data, derived from peer-reviewed reanalysis products. This indirect validation approach is consistent with established practices in agricultural meteorology and ensures the robustness of our conclusions regarding spatiotemporal patterns of climatic potential productivity in Liaoning.

However, it should be noted that these models are fundamentally a statistical model. In practical applications, it essentially represents a simple regression between vegetation productivity and environmental factors, lacking a solid foundation in physiological and ecological mechanisms. The model output represents the "annual-scale average climate potential productivity" and does not incorporate the effects of intra-annual extreme weather events, such as extreme summer heatwaves, severe spring droughts during planting periods, or intense precipitation during flood seasons. Moreover, the temporal distribution patterns of temperature and precipitation significantly influence biomass accumulation across different vegetation types. As a result, variations in temperature, humidity, and their interactions can lead to markedly different ecological outcomes. To effectively apply the Miami model and the Thornthwaite Memorial model in exploring how climate

change affects the production potential of various vegetation types, it is essential to revise and improve these climate production potential models. This improvement should involve incorporating additional meteorological variables—such as sunshine duration, relative humidity, wind speed, and soil temperature and moisture—as well as soil properties, atmospheric CO_2 concentration, and plant-specific biological factors [57].

From 1950 to 2023, the standard climate potential productivity (Yb) in Liaoning Province consistently underestimated actual production potential, with this underestimation intensifying over time. Over the past two decades, the gap has widened due to rising atmospheric CO_2 concentrations and expanded irrigation coverage. Elevated CO_2 levels have enhanced photosynthetic efficiency and water use efficiency in C3 crops, an effect that has become increasingly significant in recent years. However, the Miami/Thornthwaite model does not account for CO_2 fertilization, capturing climatic influences only through temperature and precipitation. As a result, it may systematically underestimate standard climate potential productivity and fail to reflect real growth potential. Meanwhile, solar radiation in Liaoning has followed a "decline-then-recovery" trend in recent decades, with fluctuations directly affecting Yb. Yet, the model indirectly represents radiation via temperature, potentially misattributing trend drivers—a limitation particularly evident in arid and semi-arid regions. Additionally, while advances in irrigation infrastructure and expanded irrigated areas have alleviated precipitation constraints, and crop breeding has improved stress tolerance and photosynthetic performance, the model assumes rain-fed agriculture and ignores the effects of irrigation, soil variability, and genetic improvements. This assumption amplifies spatial and temporal biases in estimated productivity. Furthermore, the model produces annual average estimates of climate-driven production potential but does not incorporate intra-annual extreme weather events—such as summer heatwaves, spring planting droughts, or heavy rainfall during flood seasons—thereby limiting its ability to capture yield variability within a single growing year.

Based on the research findings regarding the spatiotemporal dynamics and water constraints affecting Liaoning Province's standard climate potential productivity, along with an assessment of current agricultural water management strategies, the following implementation recommendations are proposed to provide practical guidance for regional agriculture in adapting to climate change and enhancing production potential. For regional resource allocation: In the low-productivity northwest zone, align interventions with the Implementation Plan for Provincial Black Soil Conservation Projects in Liaoning Province by 2025, prioritizing integrated measures of soil improvement and small-scale irrigation development. In the high-productivity southeast zone, integrate efforts with ongoing renovation plans for large- and medium-sized irrigation districts, directing investments toward smart irrigation systems and climate risk early-warning infrastructure. For cross-regional resource redistribution: leverage major water source projects to mitigate drought and alleviate water scarcity. Technology dissemination should follow the provincially validated "government + implementing entities + demonstration" model, refining region-specific pathways for promoting drought-tolerant crop varieties and rainwater harvesting techniques to ensure policy coherence and operational feasibility. To address the model's limitation in accounting for intra-annual extreme weather events, two improvement strategies are recommended: First, introduce a "Climate Resilience Index" that integrates the frequency and intensity of extreme climatic events with standard climate potential productivity, thereby establishing a dual-dimensional assessment framework encompassing both average productivity potential and extreme event risk. Second, for key maize and rice production areas in Liaoning Province, conduct panel regression analyses to quantify the relationship between extreme weather events and yield losses. This will

supplement current standard climate potential productivity assessments with an "extreme risk correction factor," thereby enhancing the comprehensiveness of food security evaluations.

Integrating these factors would strengthen the Miami and Thornthwaite models by advancing them toward more mechanistic frameworks for evaluating climate-driven production potential in terrestrial ecosystems, thereby indicating a critical avenue for future research.

5. Conclusions

Based on the Miami and Thornthwaite Memorial models, this study examines the spatio-temporal dynamics of climate potential productivity and its implications for grain yield potential in Liaoning Province from 1950 to 2023. The results show that standard climate potential productivity (Yb) exhibited no significant long-term trend. Temperature and precipitation were identified as the primary climatic drivers, with precipitation imposing a stronger limiting effect, highlighting water availability as a critical constraint on agricultural development in the region. Furthermore, both climate resource utilization efficiency and grain yield per unit area demonstrated an overall fluctuating but increasing trend over the study period. A significant positive correlation between these two variables suggests that improving grain yield per unit area is essential for enhancing climate resource use efficiency. However, the overall grain yield potential has declined, indicating that future production gains may be constrained if improvements rely solely on favorable climatic conditions.

Author Contributions: Conceptualization, D.S.; Validation, S.W.; Software, X.J.; Visualization, Q.Z.; Formal analysis, S.W. and Z.Y.; Methodology, D.S.; Investigation, S.W. and X.J.; Data curation, Q.Z.; Resources, Z.Y.; Writing—review and editing, Y.W.; Supervision, Y.W. and D.S.; Supervision, Y.W. and D.S.; Funding acquisition, S.W. All authors have read and agreed to the published version of the manuscript.

Funding: This work was funded by the National Key R&D Program of China (Grant No. 2023YFD1501300) and Economic Development Project of Liaoning Provincial Federation of Social Sciences (20251slybwzzkt-155).

Data Availability Statement: The data presented in this study are available in the paper.

Acknowledgments: The authors would like to thank the anonymous reviewers and editors for their valuable advices.

Conflicts of Interest: The authors declare no conflicts of interest.

References

1. World Meteorological Organization (WMO). WMO Report Documents Spiralling Weather and Climate Impacts [Press Release]. 19 March 2025. Available online: https://wmo.int/news/media-centre/wmo-report-documents-spiralling-weather-and-climate-impacts (accessed on 27 September 2025).
2. Gay, C.; Estrada, F.; Conde, C.; Eakin, H.; Villers, L. Potential impacts of climate change on agriculture: A case of study of coffee production in Veracruz, Mexico. *Clim. Change* **2006**, *79*, 259–288.
3. Kang, Y.H.; Ma, X.Y.; Khan, S. Predicting climate change impacts on maize crop productivity and water use efficiency in the loess plateau. *Irrig. Drain.* **2014**, *63*, 394–404.
4. Tang, G.P.; Li, X.B.; Fischer, G.; Prieler, S. Climate change and its impacts on China's agriculture. *Acta Geogr. Sin.* **2000**, *55*, 129–138.
5. Yang, X.G.; Chen, F.; Lin, X.M.; Liu, Z.J.; Zhang, H.L.; Zhao, J.; Li, K.N.; Ye, Q.; Li, Y.; Lv, S. Potential benefits of climate change for crop productivity in China. *Agric. For. Meteorol.* **2015**, *208*, 76–84.

6. Meng, L.I.; Yong, Z.; Wei, H. Influence of climate change on climate potential productivity in Yunnan. *Chin. J. Agrometeorol.* **2010**, *31*, 442–446.
7. Wu, R.N.; Yang, Y.; Li, X.M. Dynamic assessment and prediction of maize drought hazard in Liaoning Province under the background of climate change. *Int. J. Glob. Warm.* **2024**, *32*, 185–212.
8. Qi, L.; Wang, S.; Zhuang, Q.L.; Yang, Z.J.; Bai, S.B.; Jin, X.X.; Lei, G.Y. Spatial-temporal changes in soil organic carbon and pH in the Liaoning Province of China: A modeling analysis based on observational data. *Sustainability* **2019**, *11*, 3569.
9. Gu, H.L.; Li, J.B.; Wang, S. Multi-scenario simulation of land use/cover change and terrestrial ecosystem carbon reserve response in Liaoning Province, China. *Sustainability* **2024**, *16*, 8244.
10. Deng, K.H.; Ju, H.; Xiong, W.; Yang, X. The impacts of climate change on agriculture in China. *Chin. Agric. Sci. Bull.* **2006**, *22*, 439–441.
11. Wang, W.L.; Zhang, Z.H.; Zhou, Z.; Jia, Q.Q.; Liu, Z.J.; Zhang, S.H.; Jiao, L.M. Projecting cropland climatic potential productivity change in China under human activity and climate force. *Environ. Impact Assess. Rev.* **2025**, *115*, 108038.
12. Kukkurainen, H.I.; Sonneveld, B.G. Assessment of Sámi food security in Finnish Lapland: Climate change impacts and policy effectiveness. *Int. J. Circumpolar Health* **2025**, *84*, 2516310.
13. Elkhalfi, O.; Chaabita, R.; Ghoujdam, M.; Zahraoui, K.; Alaoui, H.E.; Belhaj, I. The Impact of Climate Change on Food Security in the Middle East and North Africa: Challenges and Adaptation Strategies. *J. Agric. Food Res.* **2025**, *21*, 101963.
14. Akter, M.M.; Nasher, N.R. Climate change impact on food security: Household-level adaptation barriers to Charland community in Bangladesh. *World Dev. Perspect.* **2025**, *37*, 100656.
15. Das, A.; Kumar, S.; Kasala, K.; Nedumaran, S.; Paithankar, P.; Kumar, A.; Jain, A.; Avinandan, V. Effects of climate change on food security and nutrition in India: A systematic review. *Curr. Res. Environ. Sus.* **2025**, *9*, 100286.
16. Constantinidou, K.; Hadjinicolaou, P.; Zittis, G.; Lelieveld, J. Effects of climate change on the yield of winter wheat in the eastern Mediterranean and Middle East. *Clim. Res.* **2016**, *69*, 129–141.
17. Savin, I.Y.; Stolbovoy, V.; Savitskaya, N. Climatic potential for winter wheat yield in Russia. *Russ. Agricult. Sci.* **2017**, *43*, 296–299.
18. Jevtić, R.; Župunski, V.; Lalošević, M.; Župunski, L. Predicting potential winter wheat yield losses caused by multiple disease systems and climatic conditions. *Crop Prot.* **2017**, *99*, 17–25.
19. Lu, B.Y.; Yang, B.; Fei, Z.J.; Shi, F.H.; Wang, L.; Gao, Y.B.; Liu, J. Spatial and temporal evolution of climatic productivity potential in Heilongjiang Province. *Ecol. Environ. Sci.* **2017**, *26*, 1659–1664.
20. Du, G.M.; Ma, J.P.; Zhang, L.Y.; Sun, X.B.; Zhang, Z.Y.; Liu, Z. Spatiotemporal characteristics of grain potential productivity change under the background of climate change over the past 50 years in the Sanjiang Plain. *Res. Soil. Water Conserv.* **2018**, *25*, 361–366.
21. Wang, J.R.; Zheng, J.; Su, J.; Zheng, B.H.; Sun, Z.Q. Inconsistent increasing of climate potential productivity resulting from global warming and land use transitions in the Dongting Lake Basin, from 2000 to 2020. *J. Mt. Sci.* **2023**, *20*, 1954–1967.
22. Miller, R.S. *Fundamentals of Ecology*; Wiley: Hoboken, NJ, USA, 1954; Volume 5, pp. 134–136.
23. Lieth, H.; Whittaker, R.H. (Eds.) *Primary Productivity of the Biosphere*; Springer Science & Business Media: Berlin/Heidelberg, Germany, 2012.
24. Chen, G.N. Preliminary study on calculation of primary production of ecosystem in china with application of miami model. *J. Nat. Resour.* **1987**, *2*, 270–278.
25. Lieth, H. Primary production: Terrestrial ecosystems. *Hum. Ecol.* **1973**, *1*, 303–332.
26. Austin, K.; Beach, R.; Lapidus, D.; Salem, M.; Ujeneza, N. Impacts of climate change on the potential productivity of eleven staple crops in rwanda. *Sustainability* **2020**, *12*, 4116.
27. Zheng, Z.Y. Progress of research on land use potential in China. In *Proceedings of the World Soil Resources Reports*; FAO: Beijing, China, 1994.
28. Hou, G.L. To calculate China's plant-climate productive potentialities by" Chikuzo Model. *J. Nat. Resour.* **1990**, *5*, 60–65.
29. Uchijima, Z.; Seino, H. Agroclimatic evaluation of net primary productivity of natural vegetations. *J. Agric. Meteorol.* **1985**, *40*, 343–352.
30. Yongqiang, C.; Liting, Y.; Shuang, Z.; Ming, G.; Siran, L. Trend variation and spatial characteristics of extreme climate events in Liaoning province in recent 50 years. *Water Resour. Hydropower Eng.* **2018**, *49*, 45–53.
31. Peng, S.; Gang, C.; Cao, Y.; Chen, Y. Assessment of climate change trends over the Loess Plateau in China from 1901 to 2100. *Int. J. Climatol.* **2018**, *38*, 2250–2264.

32. Adams, B.; White, A.; Lenton, T.M. An analysis of some diverse approaches to modelling terrestrial net primary productivity. *Ecol. Model.* **2004**, *177*, 353–391.
33. Lieth, H.; Box, E. Evapotranspiration and primary productivity! c.w thornthwaite memorial model. *Climatology* **1972**, *25*, 37–46.
34. Lieth, H. Modeling the primary productivity of the world. In *Primary Productivity of the Biosphere*; Springer: New York, NY, USA, 1975; pp. 237–263.
35. Tao, F.L.; Zhang, Z.; Yokozawa, M. Dangerous levels of climate change for agricultural production in China. *Reg. Environ. Change* **2011**, *11*, 41–48.
36. Mehmood, K.; Anees, S.A.; Rehman, A.; Rehman, N.U.; Muhammad, S.; Shahzad, F. Assessment of climatic influences on net primary productivity along elevation gradients in temperate ecoregions. *Trees For. People* **2024**, *18*, 100657.
37. Numajiri, H. The approximate method to estimate potential evapotranspiration using monthly mean temperature. *J. Jpn. Assoc. Hydrol. Sci.* **2006**, *36*, 71–79.
38. Zhao, H.Y.; Tian, B.X.; Gong, L.J.; Qu, H.H.; Ji, S.T.; Li, X.F.; Zhang, X.L. Climate-induced potential productivity of forest vegetation during the past 308 years in northern Da Hinggan Mountain region, China. *Acta Ecol. Sin.* **2017**, *37*, 1900–1911.
39. Kong, F.L.; Li, T.L.; Zhang, W.; Yin, P.J.; Liu, F.; Lan, T.Q.; Feng, D.J.; Wang, X.L.; Yuan, J.C. Improvement of climate resource utilization in the southwestern hilly region through the construction of a new multi-maturing cropping system. *Agronomy* **2024**, *14*, 1154.
40. Liu, W.; Sang, T. Potential productivity of the miscanthus energy crop in the loess plateau of china under climate change. *Environ. Res. Lett.* **2013**, *8*, 4003.
41. Gong, L.J.; Liu, D.; Jiang, L.Q.; Li, X.F.; Lv, J.J. Distribution characteristics of climate potential productivity of soybean in frigid region and its response to climate change. *Environ. Sci. Pollut. Res.* **2022**, *29*, 7452–7464.
42. Lobell, D.B.; Cassman, K.G.; Field, C.B. Crop yield gaps: Their importance, magnitudes, and causes. *Annu. Rev. Environ. Resour.* **2009**, *34*, 179–204.
43. Kliengchuay, W.; Mingkhwan, R.; Kiangkoo, N.; Suwanmanee, S.; Sahanavin, N.; Kongpran, J.; Aung, H.W.; Tantrakarnapa, K. Analyzing temperature, humidity, and precipitation trends in six regions of Thailand using innovative trend analysis. *Sci. Rep.* **2024**, *14*, 7800.
44. Dan'azumi, S.; Mamudu, L.; Aldrees, A. Climate change detection and attribution: Bayesian estimation of abrupt change, seasonality and trend model, and Mann–Kendall trend test approaches. *J. Water Clim. Chang.* **2025**, *16*, 1895–1911.
45. Gupta, L.K.; Verma, S. Rainfall and temperature trend analysis using mann-kendall and sen's slope estimator test in Kharun Watershed, Chhattisgarh, India. *Curr. J. Appl. Sci. Technol.* **2023**, *42*, 1–9.
46. Li, X.S.; Zheng, C.L.; Cao, C.Y.; Dang, H.K.; Sun, J.S.; Li, K.J.; Ma, J.Y. Analysis of climatic potential productivity and wheat production in different producing areas of the northern hemisphere. In Proceedings of the IOP Conference Series: Earth and Environmental Science, Beijing, China, 23–26 October 2020.
47. Hirsch, R.M.; Slack, J.R.; Smith, R.A. Techniques of trend analysis for monthly water quality data. *Water Resour. Res.* **1982**, *18*, 107–121.
48. TO, A.; SA, A.; PI, N. The impact of climate change on composition of agricultural output in Nigeria. *Am. J. Environ. Prot.* **2015**, *3*, 44–47.
49. Zhan, T.; Zhuoran, L.; Jun, S.; Fisher, G.; Tingting, G. Analysis of impact on china wheat potential productivity of climate change during 1961–2010. *Chin. Agric. Sci. Bull.* **2013**, *29*, 61–69.
50. Huang, W.H.; Yang, X.G.; Li, M.S.; Zhang, X.Y.; Wang, M.T.; Dai, S.W.; Ma, J.H. Evolution characteristics of seasonal drought in the south of China during the past 58 years based on standardized precipitation index. *Trans. Chin. Soc. Agric. Eng.* **2010**, *26*, 50–59.
51. Guo, P.P.; Yang, D.; Wang, H.; Cheng, J.Q. Climate change and its effects on climatic productivity in the Three River Headwaters Region in 1960-2011. *Chin. J. Ecol.* **2013**, *32*, 2806.
52. Norzagaray Campos, M.; Muñoz Sevilla, P.; Montiel Montoya, J.; Llanes Cárdenas, O.; Ladrón de Guevara Torres, M.; Serrano García, L.A. Rainfall potential and consequences on structural soil degradation of the most important agricultural region of Mexico. *Atmosphere* **2024**, *15*, 581.
53. Bommaraboyina, P.R.; Daniel, J.; Abbhishek, K. Book review: Climate change and agriculture in India: Impact and adaptations. *Front. Clim.* **2020**, *2*, 576004.
54. Wang, S.; Bian, S.; Wang, Z.; Yang, Z.; Li, C.; Zhang, X.; Shi, D.; Liu, H. Three-Dimensional Modeling of Soil Organic Carbon Stocks in Forest Ecosystems of Northeastern China Under Future Climate Warming Scenarios. *Forests* **2025**, *16*, 1209.

55. Wang, S.; Zhang, X.; Zhuang, Q.; Yang, Z.; Wang, Z.; Li, C.; Jin, X. Spatio-Temporal Variations in Soil Organic Carbon Stocks in Different Erosion Zones of Cultivated Land in Northeast China Under Future Climate Change Conditions. *Agronomy* **2025**, *15*, 2459.
56. Liu, J.; Pan, Y.H.; Wang, P.H.; Li, Y.M.; Jin, L.; Wen, Y.J.; Gao, S.X. Spatial and temporal characteristics of climatic potential productivity of maize in Liaoning Province from 1966 to 2015. *Chin. J. Ecol.* **2018**, *37*, 3396.
57. Tang, G.L.; Ding, Y.H.; Wang, S.W.; Ren, G.Y.; Zhang, L. Comparative analysis of the time series of surface air temperature over China for the last 100 years. *Adv. Cli. Change Res.* **2009**, *5*, 71–78.